Saturated absorption spectroscopy using diode-laser phase noise

R. Walser,* J. Cooper, and P. Zoller
Joint Institute for Laboratory Astrophysics, University of Colorado, Boulder, Colorado 80309-0440
(Received 6 April 1994)

We have investigated theoretically the applicability of phase-fluctuating laser fields in saturated absorption spectroscopy. The fluctuations of pump and probe fields are fully correlated if they are derived from the same laser source. Inside the saturable medium, phase fluctuations are converted into intensity noise. This nonlinear mixing modifies the statistics of the transmitted fields. By measuring higher-order correlations one can deduce additional spectroscopic information. Apart from the mean intensity, we have examined the intensity noise and intensity power spectrum of the weak probe field. The resonances of these correlation functions are also unaffected by large inhomogeneous broadening since they are inherently related to the usual saturated absorption dip. We find qualitative agreement with results of a recent experiment employing this technique [D.H. McIntyre *et al.*, Opt. Lett. **18**, 1816 (1993)], which demonstrates the advantages of noise spectroscopy using spectrum analyzers.

PACS number(s): 42.62.Fi, 42.60.−v, 42.65.−k, 42.25.Bs

I. INTRODUCTION

Nonlinear optical phenomena have attracted attention since the advent of laser technology, either as being fundamental to laser operation itself or by arising naturally in all applications involving high intensity fields. Among the many nonlinear effects that are employed in laser spectroscopy [1], saturated absorption is one of the most prominent. The ability to saturate selectively certain velocity groups of atoms in an inhomogeneously broadened ensemble is of major importance because it is the key mechanism involved in hole-burning spectroscopy.

In this article we will present a variation of saturated absorption spectroscopy which not only resolves spectral resonances much better than the inhomogeneous linewidth, but also has other attractive features. The method is based on the inherent characteristics of diode lasers, which have amplitudes that are, generally speaking, stable compared with those of other laser types [2], but phases that change erratically. Instead of eliminating this laser noise, we take advantage of it and extract additional information from the transmitted signal by examining not only the mean value, but also its correlations with respect to time or the power spectrum of the transmitted intensity. These quantities may be conveniently measured experimentally (e.g., by a spectrum analyzer).

The fact that higher-order correlation functions of stochastic observables are very sensitive to the statistics of the incident field has been studied thoroughly during the past few years [3–7]. The method we describe here has been used previously in saturated absorption spectroscopy measurements [8, 9]. However there have been no detailed theoretical descriptions going beyond the weak saturation regime, which we rectify with this article. In this context we have also investigated recently the influence of different statistics of the incident field on the transmitted intensity after passing through an absorption cell [10].

This article is organized as follows. In Sec. II we will state the basic relations of saturated absorption spectroscopy. Starting from the Maxwell-Bloch equations we calculate the transmitted fields within the appropriate limits. The basic features of a phase diffusing, stochastic field are introduced next. Finally, we define the observables that are discussed in Sec. III, i.e., the mean probe intensity, the intensity noise, and the intensity power spectrum. In this section we present the results of the stochastic averaging and discuss the Doppler width free resonance of the absorption coefficient. Numerical Doppler averaging of intensity noise and power spectrum then reveals similar Doppler width free structures.

II. SATURATED ABSORPTION SPECTROSCOPY

A. Maxwell-Bloch equations

The most common geometry for saturation spectroscopy (shown in Fig. 1) uses an electric field which consists of two frequency degenerate counterpropagating waves. The positive frequency part of the field is thus given by

$$\mathbf{E}^{(+)}(z,t)=\boldsymbol{\epsilon}\Big\{\varepsilon_{\mathrm{R}}(z,t)\exp\left[-i(\omega t-kz)\right]+\varepsilon_{\mathrm{L}}(z,t)\exp\left[-i(\omega t+kz)\right]\Big\}. \tag{1}$$

Here $\varepsilon_{\mathrm{R}}(z,t)$ [$\varepsilon_{\mathrm{L}}(z,t)$] is the slowly varying complex envelope of the field propagating to the right [left], $\boldsymbol{\epsilon}$ is a

*Permanent address: Institut für Theoretische Physik, Universität Innsbruck, A-6020 Innsbruck, Austria.

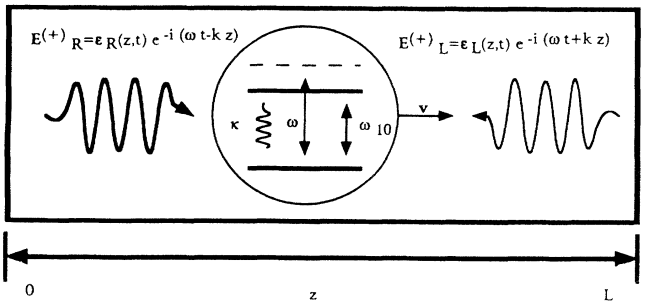

FIG. 1. Setup for saturated absorption spectroscopy with two frequency degenerate counterpropagating waves. The examined medium is described by two-level atoms.

polarization vector, and ω and $|k|$ denote the frequency and the magnitude of the wave vector, respectively. The source term of Maxwell's equation is proportional to the atomic polarization density $\mathbf{P}^{(+)}(z,t)$. Since we are especially interested in the attenuation of the right- and left-running electric fields components, we assume that the polarization density is also of this form

$$\mathbf{P}^{(+)}(z,t) = \left\langle \boldsymbol{\mathcal{P}}_R^{(+)}(z,t;v) \right\rangle_v \exp\left[-i(\omega t - kz)\right] + \left\langle \boldsymbol{\mathcal{P}}_L^{(+)}(z,t;v) \right\rangle_v \exp\left[-i(\omega t + kz)\right]. \quad (2)$$

For an inhomogeneously broadened medium we have to average the polarization density over the Doppler distribution; this is indicated by the velocity average $\langle \cdots \rangle_v = \int_{-\infty}^{\infty} (\cdots) K(v)\, dv$ with

$$K(v) = \left[k/(\sqrt{\pi} D)\right] \exp\left[-(kv/D)^2\right] \quad (3)$$

the Maxwell-Boltzmann distribution. The Doppler width D is related to the temperature of the gas by $D = \sqrt{2k_B T/m}$.

$$\left[\left(\frac{\partial}{\partial t} + v\frac{\partial}{\partial z}\right) - \begin{pmatrix} i\omega_{10} - \gamma & 0 & i\frac{\Omega^*(z,t)}{2} \\ 0 & -i\omega_{10} - \gamma & -i\frac{\Omega(z,t)}{2} \\ i\Omega(z,t) & -i\Omega^*(z,t) & -\kappa \\ 0 & 0 & 0 \end{pmatrix}\right] \begin{pmatrix} \rho_{01}(z,t;v) \\ \rho_{10}(z,t;v) \\ w(z,t;v) \\ tr(z,t;v) \end{pmatrix} = 0 \quad (7)$$

with a Rabi frequency $\Omega(z,t) = \Omega_R(z,t) \exp\left[-i(\omega t - kz)\right] + \Omega_L(z,t) \exp\left[-i(\omega t + kz)\right]$, where $\Omega_R(z,t) = 2\boldsymbol{\epsilon} \cdot \mathbf{D}_{10}\, \varepsilon_R(z,t)/\hbar$ and $\Omega_L(z,t) = 2\boldsymbol{\epsilon} \cdot \mathbf{D}_{10}\, \varepsilon_L(z,t)/\hbar$. The atomic transition frequency is denoted by ω_{10} while κ is the spontaneous emission rate. The population inversion is called $w(z,t;v) = \rho_{11}(z,t;v) - \rho_{00}(z,t;v)$ and the trace $\mathrm{tr}(z,t;v) = \rho_{11}(z,t;v) + \rho_{00}(z,t;v) \equiv 1$ is conserved.

Since we have already assumed that the medium is dilute we can further simplify the ensuing treatment by approximating the local Rabi frequency with the Rabi frequency in the absence of absorption $\Omega_R(z,t) \approx \Omega_{R_{\mathrm{in}}}(t - z/c) \approx \Omega_{R_{\mathrm{in}}}(t)$. This will lead to results to lowest order in the absorption coefficient [9, 10]. The second approximate equivalence stems from the fact that the propagation time through the medium is in general much less than the correlation time of the field ($L/c \ll \tau_c$). An analogous relation holds for the field propagating to the left.

By formally integrating Maxwell's equation in one dimension and within the slowly varying envelope approximation, we relate the output field of the right-running component $\boldsymbol{\varepsilon}_{R_{\mathrm{out}}}(t) \equiv \varepsilon_R(z = L, t)$ and the input field $\varepsilon_{R_{\mathrm{in}}}(t) \equiv \varepsilon_R(z = 0, t)$ through

$$\varepsilon_{R_{\mathrm{out}}}(t) = \varepsilon_{R_{\mathrm{in}}}(t_{\mathrm{ret}}) + \frac{ik}{2\varepsilon_0} \times \int_0^{z=L} dz' \left\langle \boldsymbol{\epsilon}^* \cdot \boldsymbol{\mathcal{P}}_R^{(+)}(z', t_{\mathrm{ret}} + z'/c; v) \right\rangle_v, \quad (4)$$

and similarly for the field component propagating to the left

$$\varepsilon_{L_{\mathrm{out}}}(t) = \varepsilon_{L_{\mathrm{in}}}(t_{\mathrm{ret}}) - \frac{ik}{2\varepsilon_0} \int_L^{z=0} dz' \times \langle \boldsymbol{\epsilon}^* \cdot \boldsymbol{\mathcal{P}}_L^{(+)}(z', t_{\mathrm{ret}} + (L - z')/c; v) \rangle_v, \quad (5)$$

with $\varepsilon_{L_{\mathrm{out}}}(t) \equiv \varepsilon_L(z = 0, t)$, $\varepsilon_{L_{\mathrm{in}}}(t) \equiv \varepsilon_L(z = L, t)$, and a retarded time $t_{\mathrm{ret}} = t - L/c$.

In a semiclassical description the polarization density $\mathbf{P}^{(+)}(z,t)$ is proportional to the expectation value of the induced dipole moment. For a medium of two-level atoms with ground state $|0\rangle$ and excited state $|1\rangle$ the polarization density within a small volume dV containing $dN = n\, dV$ two-level atoms is

$$\mathbf{P}^{(+)}(z,t)\, dV = 2 \langle \mathbf{D}_{01}\, \rho_{10}(z,t;v) \rangle_v\, dN, \quad (6)$$

with $\mathbf{D}_{01}$ the atomic dipole between ground and excited states and $\rho_{10}(z,t;v)$ the atomic dipole coherence of a single atom moving with velocity v.

If the probability of inelastic, velocity, or velocity-direction changing collisions is low, as is the case in a dilute gas, then the atoms will move along linear paths with velocity v. However, the decay rate of the induced dipole moment γ is increased due to frequent elastic, but dephasing, encounters with other atoms. Consequently, we find for the time evolution of a single moving two-level atom

B. Stochastic laser fields

The laser fields $\varepsilon_{R_{\mathrm{in}}}(t)$ and $\varepsilon_{L_{\mathrm{in}}}(t)$ incident at the left- and right-hand sides of the vapor cell are derived from the same laser source. The optical path lengths are adjusted so that they will differ just in magnitude ($|\eta| \ll 1$) and constant phase $\varepsilon_{L_{\mathrm{in}}}(t) = \eta\, \varepsilon_{R_{\mathrm{in}}}(t)$. To observe saturated absorption the field propagating to the right has to be saturating while the counterpropagating field is just a weak probe beam.

The field intensity emitted by a single mode diode laser is very stable compared to other laser types [2]. However, the instantaneous phase is changing erratically. This can be modeled by a field with a constant amplitude and a stochastic phase $\varepsilon(t) = \varepsilon\, e^{-i\phi(t)}$, which implies that there are no intensity fluctuations.

If the phase changes in a continuous way with a low probability of large instantaneous phase changes, and if the field spectrum is Lorentzian with a bandwidth b, i.e., $\langle\langle \varepsilon e^{-i\phi(t_1)}\varepsilon^* e^{i\phi(t_2)}\rangle\rangle = |\varepsilon|^2 e^{(-b|t_1-t_2|)}$, then this can be described by a Wiener process [11] which has zero mean $\langle\langle d\phi(t)\rangle\rangle = 0$ and variance of $\langle\langle [d\phi(t)]^2\rangle\rangle = 2b\,dt$. The angular brackets $\langle\langle\ \rangle\rangle$ denote the stochastic average. This is usually referred to as a "phase diffusing field" (PDF).

C. The weak probe absorption coefficient

The left- and right-propagating waves cause a spatial modulation of the population inversion due to the position-dependent intensity. Multiple backward and forward scattering is induced by this index grating so that it is necessary to decompose the polarization and the inversion into Fourier components:

$$\rho_{10}(z,t;v) = \sum_m \eta^{|m|}\rho_{10}^{(m)}(t;v)e^{-i[\omega t-(2m+1)kz]}, \quad (8)$$

$$\rho_{01}(z,t;v) = \sum_m \eta^{|m|}\rho_{01}^{(m)}(t;v)e^{i[\omega t-(2m+1)kz]}, \quad (9)$$

$$w(z,t;v) = \sum_m \eta^{|m|}w^{(m)}(t;v)e^{i2mkz}, \quad (10)$$

$$tr(z,t;v) = 1, \quad (11)$$

where the weak probe Rabi frequency $|\Omega_L|$ is well below the saturation limit $\Omega_{\rm sat}$, so that $\eta = |\Omega_L|/\Omega_{\rm sat}$ can serve as an expansion parameter. Note that η is space and time independent for a PDF $[\Omega_{L,R}(t) = |\Omega_{L,R}|\, e^{-i\phi(t)}]$. After substituting this ansatz into the Bloch equation (7) and discarding second-order contributions we find

$$\left[\frac{\partial}{\partial t} - e^{-i\underline{N}\phi(t)}\underline{\tilde{A}}e^{i\underline{N}\phi(t)}\right]\mathbf{u}(t;v) = \mathbf{0}, \quad (12)$$

$$\underline{\tilde{A}} = \begin{pmatrix} \underline{A}_{4\times4}(|\Omega_R|) & \mathbf{0}_{4\times6} \\ \underline{C}_{6\times4}(\eta\Omega_{\rm sat}) & \underline{B}_{6\times6}(|\Omega_R|)\end{pmatrix}, \quad (13)$$

$$\mathbf{u}(t;v) = \begin{pmatrix}\mathbf{u}_0(t;v)\\ \mathbf{u}_1(t;v)\end{pmatrix},$$

with $\mathbf{u}_0(t;v) = [w^{(0)}(t;v), \rho_{01}^{(0)}(t;v),\ \rho_{10}^{(0)}(t;v), \mathrm{tr}]^T$ and $\mathbf{u}_1(t;v) = \eta[\rho_{01}^{(-1)}(t;v),\ \rho_{10}^{(-1)}(t;v),\ w^{(1)}(t;v),\ w^{(-1)}(t;v),\ \rho_{01}^{(1)}(t;v),\ \rho_{10}^{(1)}(t;v)]^T$. The matrix $\underline{A}_{4\times4}$ and the Bloch vector $\mathbf{u}_0(t;v)$ describe the behavior of an atom in the absence of a counterpropagating beam. The explicit definitions of the submatrices $\underline{A}, \underline{B}, \underline{C}$ and the diagonal matrix $\underline{N}$ are given in the appendix.

Finally, we can calculate the weak probe field that is emitted at the left-hand side at $z = 0$ as

$$\varepsilon_{L_{\rm out}}(t) = \varepsilon_{L_{\rm in}}(t_{\rm ret}) + i(\alpha_L L)\sqrt{\langle\langle \varepsilon_{L_{\rm in}}\varepsilon^*_{L_{\rm in}}\rangle\rangle}\left\langle \rho_{10}^{(-1)}(t_{\rm ret};v)\right\rangle_v, \quad (14)$$

where we have defined a dimensionless attenuation parameter as $(\alpha_L L) = n(kL)\varepsilon^*\mathbf{D}_{01}\eta/(\varepsilon_0\sqrt{\langle\langle \varepsilon_{L_{\rm in}}\varepsilon^*_{L_{\rm in}}\rangle\rangle})$. Within the weak absorption regime it is required to be much smaller than unity.

The transmitted intensity measured by a detector at $z = 0$ is $I_{L,\rm out}(t) = 2c\varepsilon_0\ \varepsilon_{L_{\rm out}}(t)\ \varepsilon_{L_{\rm out}}(t)^*$ and consists mainly of the incident intensity $I_{L,\rm in}$ which is a constant in the present model, and the absorbed intensity defined as

$$I_{L,abs}(t;v) = i\,2c\varepsilon_0\sqrt{\langle\langle \varepsilon_{L_{\rm in}}\varepsilon^*_{L_{\rm in}}\rangle\rangle}\,\varepsilon_{L_{\rm in}}(t)^*\rho_{10}^{(-1)}(t;v) + \text{c.c.}, \quad (15)$$

so that

$$I_{L,\rm out}(t) = I_{L,\rm in} + (\alpha_L L)\langle I_{L,\rm abs}(t_{\rm ret};v)\rangle_v + \mathcal{O}[(\alpha_L L)^2]. \quad (16)$$

However, this is still a fluctuating quantity which has to be averaged:

$$\langle\langle I_{L,\rm out}(t)\rangle\rangle = I_{L,\rm in} + (\alpha_L L)\left\langle \langle\langle I_{L,abs}(t_{ret};v)\rangle\rangle\right\rangle_v + \mathcal{O}((\alpha_L L)^2). \quad (17)$$

The intensity fluctuations are measured by their variance (using $\langle\langle a,b\rangle\rangle = \langle\langle ab\rangle\rangle - \langle\langle a\rangle\rangle\langle\langle b\rangle\rangle$)

$$\Delta^2 I_{L,\rm out}(t) = (\alpha_L L)^2\,\langle\langle I_{L,\rm abs}(t_{\rm ret};v_1), I_{L,\rm abs}(t_{\rm ret};v_2)\rangle\rangle\rangle_{v_1,v_2} + \mathcal{O}((\alpha_L L)^3) \quad (18)$$

and the stationary power spectrum of the intensity fluctuations of the transmitted field (as measured by, for example, a spectrum analyzer)

$$S_{\rm out}(\nu) = (\alpha_L L)^2 \lim_{t\to\infty} 2\mathrm{Re}\int_0^\infty e^{-i\nu\tau}\left\langle \langle\langle I_{L,\rm abs}(t+\tau;v_1), I_{L,\rm abs}(t;v_2)\rangle\rangle\right\rangle_{v_1,v_2} d\tau + \mathcal{O}((\alpha_L L)^3). \quad (19)$$

No constant $(\alpha_L L)^0$ or linear contributions $(\alpha_L L)^1$ appear in Eqs. (19) and (18). These terms vanish identically in the case of a phase fluctuating field. Note also the double velocity average.

The stochastic averages that are required to determine the mean intensity are $\langle\langle \mathbf{g}_1(t;v)\rangle\rangle$ with $\mathbf{g}_1(t;v) = e^{i\underline{N}\phi(t)}\mathbf{u}(t;v)$ and the covariance matrix $\underline{c}_2(t;v_1,t;v_2) = \langle\langle \underline{g}_2(t;v_1,t;v_2)\rangle\rangle - \langle\langle \mathbf{g}_1(t;v_1)\rangle\rangle\langle\langle \mathbf{g}_1(t;v_2)\rangle\rangle^\dagger$ with $\underline{\mathbf{g}}_2(t;v_1,t;v_2) = \mathbf{g}_1(t;v_1)\mathbf{g}_1(t;v_2)^\dagger$. The power spectrum is derived from the Laplace transform of the covariance matrix $\underline{c}_2(s = i\nu;v_1,v_2) =$

$\lim_{t\to\infty}\mathcal{L}_s[\underline{c}_2(\bar{t};v_1,t;v_2)]$. These averages can be evaluated analytically and in closed form (for instance, see [11] or Appendix B of [10]). We obtain, for the stationary values,

$$0=[\tilde{\underline{A}}(v)-b\underline{N}^2]\langle\langle\underline{\mathbf{g}}_1(t;v)\rangle\rangle_{t\to\infty}, \tag{20}$$

$$\begin{aligned}0=&[\tilde{\underline{A}}(v_1)-b\underline{N}^2]\left\langle\left\langle\underline{\mathbf{g}}_2(t;v_1,t;v_2)\right\rangle\right\rangle_{t\to\infty}\\&+\left\langle\left\langle\underline{\mathbf{g}}_2(t;v_1,t;v_2)\right\rangle\right\rangle_{t\to\infty}[\tilde{\underline{A}}^{\dagger}(v_2)-b\underline{N}^2]\\&+2b\,\underline{N}\left\langle\left\langle\underline{\mathbf{g}}_2(t;v_1,t;v_2)\right\rangle\right\rangle_{t\to\infty}\underline{N},\end{aligned} \tag{21}$$

and

$$\begin{aligned}\underline{c}_2(s=i\nu;v_1,v_2)=&\{i\,\nu-[\tilde{\underline{A}}(v_1)-b\underline{N}^2]\}^{-1}\\&\times\underline{c}_2(t;v_1,t;v_2)_{t\to\infty}\,.\end{aligned} \tag{22}$$

III. DISCUSSION

The intensity that is absorbed from the left running probe field is proportional to the rate $\mathrm{Im}\{\Omega_L^*(t)\rho_{10}^{(-1)}(t;v)\}$. This rate consists of two distinct contributions as given by

$$\begin{aligned}\rho_{10}^{(-1)}(t;v)=\left(\frac{i}{2}\right)\int_{-\infty}^{t}e^{Z_{(-1)}^*(t-t_1)}\Big[&\Omega_L(t_1)w^{(0)}(t_1;v)\\&+\Omega_R(t_1)w^{(-1)}(t_1;v)\Big],\end{aligned} \tag{23}$$

with $Z_{(m)}=-i\,(\delta-m\,kv)-\gamma$. Their physical origin is obviously the standing wave pattern of the two counterpropagating fields. The first term is proportional to the inversion of a spatially averaged intensity. It is an incoherent contribution since the inversion is only intensity dependent; thus the coherence of the pump and probe field is of no relevance. The second term, however, reflects the spatially periodic structure of the inversion. This can be interpreted as an index grating. Hence multiple coherent scattering of pump and probe beam will occur. All of these scattering processes, which give rise to absorption of a wave propagating to the left, are contained within this second contribution (within the weak probe field limit).

To gain some insight into the processes involved, we can approximate the phase-averaged absorption rate [using Eq. (20)] for a nonsaturating pump field. Thus

$$\begin{aligned}\eta\langle\langle e^{i\phi(t)}\rho_{10}^{(-1)}(t;v)\rangle\rangle_{t\to\infty}=&\left(\frac{i}{2}\right)\frac{|\Omega_L|}{(Z_{(-1)}^*-b)}\left(-1-\frac{|\Omega_R|^2}{\kappa}\mathrm{Re}\left\{\frac{1}{Z_{(1)}-b}\right\}\right)\\&+\left(-\frac{i}{4}\right)\frac{|\Omega_R|}{(Z_{(-1)}^*-b)}\frac{|\Omega_L|}{(\kappa-2ikv)}\frac{|\Omega_R|}{(Z_{(-1)}-b)}\\&+\left(-\frac{i}{4}\right)\frac{|\Omega_R|}{(Z_{(-1)}^*-b)}\frac{|\Omega_R|}{(\kappa-2ikv)}\frac{|\Omega_L|}{(Z_{(1)}^*-b)}+\mathcal{O}\left(\left(|\Omega_R|/\Omega_{\mathrm{sat}}\right)^4\right).\end{aligned} \tag{24}$$

The first term corresponds to a depletion of the ground state due to the pump field and a subsequent generation of a left-running weak probe polarization ($w^{(0)}\overset{\Omega_R^*}{\to}\rho_{01}^{(0)}\overset{\Omega_R}{\to}w^{(0)}\overset{\Omega_L}{\to}\rho_{10}^{(-1)}$). The second term consists of a pump field coherence which gives rise to a spatial modulation of the inversion after absorption from the probe field. Finally, the pump field is scattered into the backwards direction ($w^{(0)}\overset{\Omega_R^*}{\to}\rho_{01}^{(0)}\overset{\Omega_L}{\to}w^{(-1)}\overset{\Omega_R}{\to}\rho_{10}^{(-1)}$). In the last term a left-running polarization is created by the absorption from the weak probe field. This and a pump photon spatially modulate the inversion and again the pump field is scattered backwards ($w^{(0)}\overset{\Omega_L}{\to}\rho_{10}^{(-1)}\overset{\Omega_R^*}{\to}w^{(-1)}\overset{\Omega_R}{\to}\rho_{10}^{(-1)}$).

A. Weak probe intensity

It is well known (and the basis of saturated absorption spectroscopy) that the hole burned into the velocity distribution by the pump field (at $\delta=kv$) and the resonant absorption from the weak probe field (at $\delta=-kv$) overlap at $\delta=kv=0$ and cause a resonance (Lamb dip) which is unaffected by a Doppler average. By integrating Eq. (24) over a very broad Doppler distribution [$D\gg\max(\kappa,\gamma,b,\delta,\Omega_{R,L})$] one finds that the weak probe output intensity is given approximately by

$$\begin{aligned}\langle\langle\langle I_{L,\mathrm{out}}\rangle\rangle\rangle_v=\langle\langle I_{L,\mathrm{in}}\rangle\rangle\Bigg(&1-(\alpha_L L)|\Omega_L|\frac{\sqrt{\pi}}{D}\\&\times\left[1-\frac{|\Omega_R|^2}{2\kappa}\frac{b+\gamma}{\delta^2+(b+\gamma)^2}\right]\Bigg)\\&+\mathcal{O}\left(\left(|\Omega_R|/\Omega_{sat}\right)^4\right).\end{aligned} \tag{25}$$

This demonstrates the appearance of the Doppler width free central structure.

In Fig. 2 we present the result of numerically Doppler averaging the weak probe intensity vs laser detuning δ [using Eq. (20)]. The solid ($b=0.1\kappa$), dash-dotted ($b=1\kappa$), and dashed ($b=5\kappa$) curves show the dependence on the laser bandwidth. To facilitate a qualitative comparison with the approximation discussed above [Eq. (25)] we have included it (as the dotted line with $b=1\kappa$), although it can be used with confidence only in the weak field limit while here the Rabi frequency of the pump field is already saturating $|\Omega_R|=1\kappa$. To avoid the rescaling of all numerical results, we have set the weak probe absorption coefficient to $(\alpha_L L)=1$, though, in principle, it is limited to values $(\alpha_L L)\ll 1$. The central resonance is smeared out by increasing the bandwidth (decreasing saturation). This behavior is also to be expected for dif-

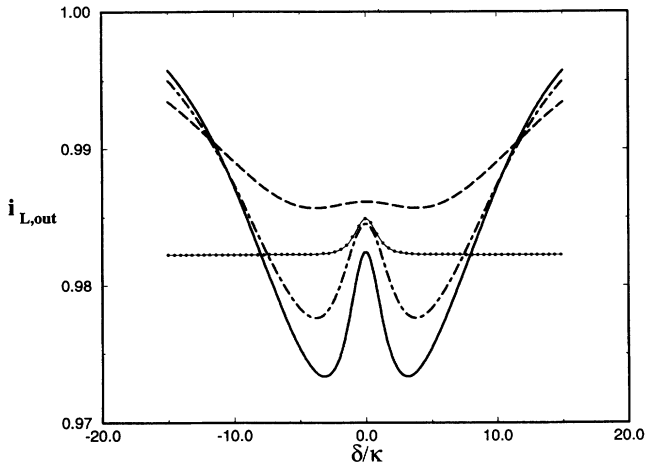

FIG. 2. Scaled mean weak probe intensity $i_{L,\mathrm{out}} = \langle\langle\langle\langle I_{L,\mathrm{out}}\rangle\rangle\rangle\rangle_v / \langle\langle I_{L,in}\rangle\rangle$ vs laser detuning δ. The solid ($b = 0.1\kappa$), dash-dotted ($b = 1\kappa$), and dashed ($b = 5\kappa$) curves show the dependence on the laser bandwidth. The dotted line represents the large Doppler width approximation [Eq. (25)] for $b = 1\,\kappa$. The other parameters are $|\Omega_R| = 1\kappa$, $|\Omega_L| = 0.1\kappa$, $\gamma = 0.5\kappa$, a Doppler width of $D = 10\kappa$, and we have set the attenuation parameter to $(\alpha_L L) = 1$.

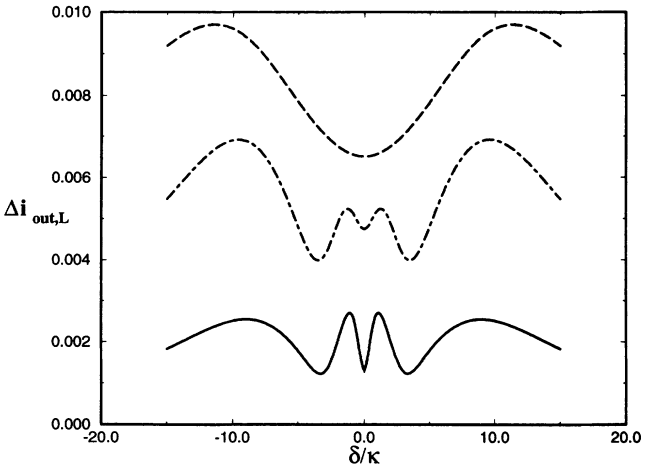

FIG. 3. Scaled standard deviation of the weak probe intensity $\Delta i_{L,\mathrm{out}}(\delta) = \sqrt{\langle\Delta^2 I_{L,\mathrm{out}}\rangle_{v_1,v_2}} / \langle\langle I_{L,\mathrm{in}}\rangle\rangle$ vs detuning for three different bandwidths: $b = 0.1\kappa$ (solid), $b = 1\kappa$ (dash-dotted), and $b = 5\kappa$ (dashed). The other parameters are the same as in Fig. 2.

ferent collision rates since the dephasing rate $b + \gamma$ is additive.

B. Induced intensity noise

In Fig. 3 we show the standard deviation of the intensity fluctuations corresponding to the situation depicted in Fig. 2. In general, the noise level rises with increasing bandwidth. The structure of the induced intensity noise can be understood easily in the limiting situation of small bandwidth. If the atoms can reach an equilibrium state before the instantaneous detuning $\delta(t) = \delta + \dot{\phi}(t)$ has altered significantly, then the transmitted intensity will change according to $d\langle\langle\langle I_{L,\mathrm{out}}(\delta(t);v)\rangle\rangle\rangle_v \approx d\delta(t)\,\frac{\partial}{\partial\delta}\langle\langle\langle I_{L,\mathrm{out}}(\delta(t);v)\rangle\rangle\rangle_v$. On resonance, or where the derivative vanishes, the intensity noise is also low, whereas it is maximal at the turning points. Larger bandwidths erase the Doppler width free structure and only the noise maxima at the turning points of the convolving Gaussian ($\delta \approx \pm D/\sqrt{2}$) remain.

C. The power spectrum of the probe field

The intensity correlation spectrum [Eq. (19)] determines the characteristic frequencies of the time evolution of the transmitted intensity. Since $I_{L,\mathrm{abs}}(t;v)$ is proportional to the absorption rate $\mathrm{Im}\{\Omega_L^*(t)\rho_{10}^{(-1)}(t;v)\}$ one can expect resonances around $\nu \approx \pm(\delta + kv)$, at least in the limit of a very weak pump field. In general, one has to invert Eq. (22), which yields

$$\begin{aligned}\langle\langle \underline{c}_2^{11}(s = i\nu; v_1, v_2)\rangle\rangle &= \{i\nu - [\underline{B}(v_1) - b\underline{N}_1^2]\}^{-1}(\langle\langle \underline{c}_2^{11}(t; v_1, t; v_2)\rangle\rangle_{t\to\infty} \\ &+ \underline{C}\{i\nu - [\underline{A}(v_1) - b\underline{N}_0^2]\}^{-1} \\ &\times \langle\langle \underline{c}_2^{01}(t; v_1, t; v_2)\rangle\rangle_{t\to\infty}) \qquad (26)\end{aligned}$$

where the submatrices $\underline{c}_2^{01}$ and $\underline{c}_2^{11}$ contain the covariance between the Bloch-vector components of order (0,1) and (1,1), respectively.

In the absence of Doppler broadening ($kv = 0$) the eigenvalues $i\,\nu_B$ of $(\underline{\mathbf{B}}(v = 0) - b\underline{N}_1^2)$ are degenerate with the eigenvalues $i\,\nu_A$ of $(\underline{\mathbf{A}}(v = 0) - b\underline{N}_0^2)$ (with the exception of the eigenvalue $\nu_A = 0$, which reflects the conservation of the trace). A finite kv removes the degeneracy of the eigenvalues, i.e., the eigenfrequencies $\Omega_A = \mathrm{Re}\{\nu_A\}$, $\Omega_B = \mathrm{Re}\{\nu_B\}$ split up while the widths $\Gamma^c = \mathrm{Im}\{\nu_A^c, \nu_B^c\}$ of coherence components $\{\rho_{01}^{(-1)}, \rho_{01}^{(0)}, \rho_{01}^{(1)}\}$ on one side and the widths $\Gamma^w = \mathrm{Im}\{\nu_A^w, \nu_B^w\}$ of the inversion components $\{w^{(-1)}, w^{(0)}, w^{(1)}\}$ on the other side remain degenerate. Though it is possible to determine the roots of the characteristic polynomials analytically, the resulting expressions are not instructive and an approximation in the case of a weak pump field reveals the facts mentioned before more clearly. Thus we find approximately

$$i\,\nu_A = \{0, -\Gamma^w, -\Gamma^c \pm i\,\Omega_A(v)\} + \mathcal{O}(\Omega_R/\Omega_{\mathrm{sat}})^4), \qquad (27)$$

$$i\,\nu_B = \{-\Gamma^w \pm 2i\,kv, -\Gamma^c \pm i\,[\Omega_A(v) + 2\,kv], -\Gamma^c \pm i\,[\Omega_A(v) - 2\,kv]\} + \mathcal{O}((\Omega_R/\Omega_{\mathrm{sat}})^4), \qquad (28)$$

with a generalized Rabi frequency $\Omega_A(v) = (\delta - kv) + \frac{\Omega_R^2}{2}\mathcal{D}(\delta - kv)$, $\Gamma^w = \kappa - \Omega_R^2\mathcal{L}(\delta - kv)$, $\Gamma^c = b + \gamma + \frac{\Omega_R^2}{2}\mathcal{L}(\delta - kv)$, and $\mathcal{L}(\delta) - i\mathcal{D}(\delta) = [(\kappa - b - \gamma) + i\delta]^{-1}$.

The results of numerically Doppler averaging the weak probe power spectrum by means of Eq. (22) can be seen in Fig. 4. There we show the intensity power spectrum $S_{\text{out}}(\nu, \delta)$ vs spectral frequency ν and keep the detuning fixed at $\delta = 5\kappa$. The solid, dash-dotted, and dashed lines correspond to bandwidths of $b = 0.1\kappa$, $b = 1\kappa$, and $b = 5\kappa$, respectively. All other parameters are the same as in Figs. 2 and 3. The dotted curve is the power spectrum in the absence of Doppler broadening ($D = 0$ and $kv = 0$) for a bandwidth of $b = 0.1\kappa$ and scaled by a factor 1/100. Its spectral resonance occurs around the generalized Rabi frequency $\nu \approx \Omega_A(v = 0) \approx 5.098\kappa$. Comparison with the numerical result for a finite Doppler width of $D = 10\kappa$ (solid line) suggests a separation of the single resonance into a dip and a peak according to the splitting of the eigenfrequencies as given by Eq. (28). But due to the complexity of the involved expressions we have not succeeded in locating them more precisely by means of a perturbative calculation as has been done for the mean absorbed intensity.

The role of detuning δ and spectral frequency ν is reversed in Fig. 5. Here we scan the laser detuning over the resonance and fix the spectral frequency at $\nu = 5\kappa$. This provides an alternative form for obtaining the spectrum, which may sometimes have practical advantages. The obtained curves closely resemble the intensity noise (Fig. 3) which is approached when $\nu \to 0$. All other parameters are the same as in Fig. 4. In addition to the central noise maxima and the maxima at the location of the steepest slopes of the convolving Gaussian, resonances appear at the spectral frequency $\delta \approx \nu = 5\kappa$.

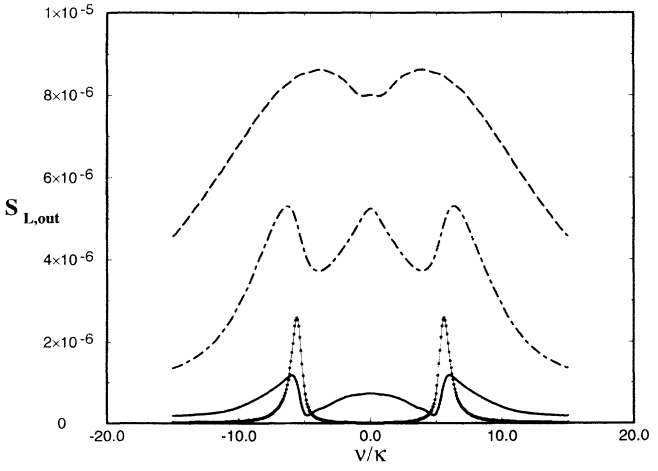

FIG. 4. The intensity power spectrum of the weak probe field $S_{L,\text{out}}(\nu, \delta)$ vs spectral frequency ν. The laser detuning is fixed at $\delta = 5\kappa$. The solid, dash-dotted, and dashed lines correspond to bandwidths of $b = 0.1\kappa$, $b = 1\kappa$, and $b = 5\kappa$. The Doppler width is $D = 10\kappa$. In the absence of Doppler broadening $D = 0$ and $b = 0.1\kappa$, the dotted line is obtained (scaled by 1/100). The other parameters are the same as in Fig. 2.

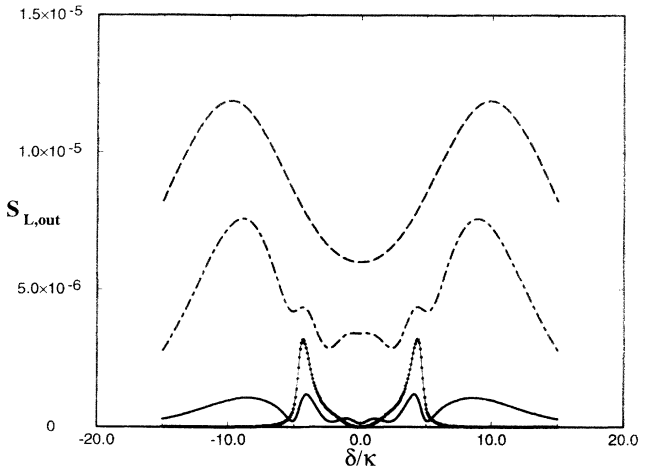

FIG. 5. The intensity power spectrum of the weak probe field $S_{L,\text{out}}(\nu, \delta)$ vs. laser detuning δ. The spectral frequency is fixed at $\nu = 5\kappa$. The solid, dashed–dotted, and dashed lines correspond to bandwidths of $b = 0.1\kappa$, $b = 1\kappa$, and $b = 5\kappa$. The Doppler width is $D = 10\kappa$. In the absence of Doppler broadening $D = 0$ and $b = 0.1\kappa$, the dotted line is obtained (scaled by 1/100). The other parameters are the same as in Fig. 2.

In Fig. 6 we also present the power spectrum vs detuning δ, but decrease the spectral frequency to $\nu = 1\kappa$. This spectrum (especially $b = 0.1\kappa$) then corresponds to the experimental setup described in Ref. [9] and is in qualitative agreement with Fig. 3 of that Letter.

IV. CONCLUSIONS

We have examined the influence of phase fluctuations on the standard configuration for saturated absorption

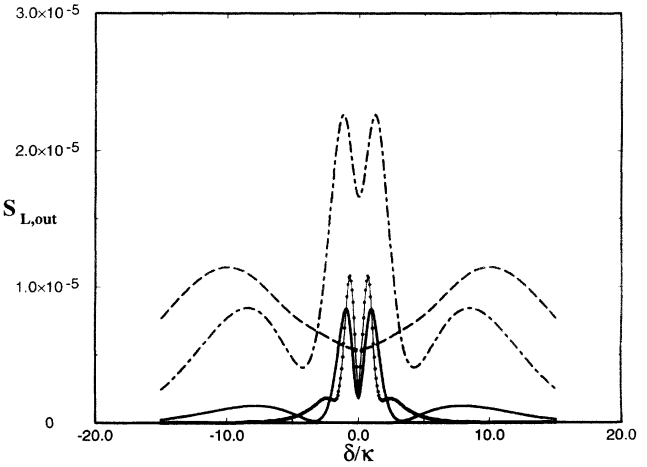

FIG. 6. The intensity power spectrum of the weak probe field $S_{L,\text{out}}(\nu, \delta)$ vs. laser detuning δ for three different bandwidths: $b = 0.1\kappa$ (solid), $b = 1\kappa$ (dashed–dotted), and $b = 5\kappa$ (dashed). The spectrum analyzer frequency is fixed to $\nu = 1\kappa$. All other parameters remain the same as in Fig. 2. In the absence of Doppler broadening $D = 0$ and $b = 0.1\kappa$, the dotted line is obtained (scaled by 1/3).

spectroscopy. The two counterpropagating laser beams are frequency degenerate and their phase fluctuations are fully correlated since they are derived from the same source. It is well known that the weak probe absorption coefficient is reduced by a saturating pump field and gives rise to the Lamb dip. This resonance is unaffected by Doppler broadening. In addition, by analyzing the laser-induced intensity fluctuations or their power spectrum we have found that they also have these Doppler width free resonances. They can be used to determine the homogeneous width or the location of the transition more precisely by exploiting the intrinsic frequency fluctuations of diode lasers rather than by attempting to eliminate them.

ACKNOWLEDGMENTS

This work has been supported in part by the National Science Foundation through grants to the University of Colorado and by the Austrian Fonds zur Förderung der Wissenschaftlichen Forschung under grant No. P7295. R. W. is also grateful for support from the Austrian Bundesministerium für Wissenschaft und Forschung.

APPENDIX: DEFINITIONS OF MATRIX COEFFICIENTS

The definitions of the matrix coefficients appearing in Eq. (12) are the following:

$$\underline{A} = \begin{pmatrix} -\kappa & i|\Omega_R| & -i|\Omega_R| & -\kappa \\ i/2|\Omega_R| & Z_1 & 0 & 0 \\ -i/2|\Omega_R| & 0 & Z_1^* & 0 \\ 0 & 0 & 0 & 0 \end{pmatrix}, \tag{A1}$$

$$\underline{B} = \begin{pmatrix} Z_{-1} & 0 & i/2|\Omega_R| & 0 & 0 & 0 \\ 0 & Z_{-1}^* & 0 & -i/2|\Omega_R| & 0 & 0 \\ i|\Omega_R| & 0 & -(\kappa + i2kv) & 0 & 0 & -i|\Omega_R| \\ 0 & -i|\Omega_R| & 0 & -(\kappa - i2kv) & i|\Omega_R| & 0 \\ 0 & 0 & 0 & i/2|\Omega_R| & Z_3 & 0 \\ 0 & 0 & -i/2|\Omega_R| & 0 & 0 & Z_3^* \end{pmatrix}, \tag{A2}$$

$$\underline{C} = i/2|\Omega_L| \begin{pmatrix} 1 & 0 & 0 & 0 \\ -1 & 0 & 0 & 0 \\ 0 & 0 & -2 & 0 \\ 0 & 2 & 0 & 0 \\ 0 & 0 & 0 & 0 \\ 0 & 0 & 0 & 0 \end{pmatrix}, \quad \underline{N} = \begin{pmatrix} \underline{N}_0 & 0 \\ 0 & \underline{N}_1 \end{pmatrix}, \tag{A3}$$

with $\underline{N}_0 = \mathrm{diag}(0,-1,1,0)$, $\underline{N}_1 = \mathrm{diag}(-1,1,0,0,-1,1)$ and $Z_m = -i\,(\delta - m\,kv) - \gamma$.

[1] For instance, see M. D. Levenson, *Introduction to Nonlinear Laser Spectroscopy* (Academic, New York, 1982) or P. Meystre and M. Sargent III, *Elements of Quantum Optics* (Springer-Verlag, Berlin, 1990).
[2] S. Machida, Y. Yamamoto, and Y. Itaya, Phys. Rev. Lett. **58**, 1000 (1987).
[3] P. Zoller, Phys. Rev. A **20**, 2420 (1979).
[4] Th. Haslwanter, H. Ritsch, J. Cooper, and P. Zoller, Phys. Rev. A **38**, 5652 (1988).
[5] M. H. Anderson, R. D. Jones, J. Cooper, S. J. Smith, D. S. Elliott, H. Ritsch, and P. Zoller, Phys. Rev. Lett. **64**, 1346 (1990).
[6] M. H. Anderson, R. D. Jones, J. Cooper, S. J. Smith, D. S. Elliott, H. Ritsch, and P. Zoller, Phys. Rev. A **42**, 6690 (1990).
[7] R. Walser, H. Ritsch, P. Zoller, and J. Cooper, Phys. Rev. A **45**, 468 (1992).
[8] T. Yabuzaki, T. Mitsui, and U. Tanaka, Phys. Rev. Lett. **67**, 2453 (1991).
[9] D. H. McIntyre, C. E. Fairchild, J. Cooper, and R. Walser, Opt. Lett. **18**, 1816 (1993).
[10] R. Walser and P. Zoller, Phys. Rev. A **49**, 5067 (1994).
[11] C. W. Gardiner, *Handbook of Stochastic Methods* (Springer, Berlin, 1990)